A Time-of-Flight Spectrometer for Measuring Inelastic to Mastic Differential Cross Section Ratios for Electron-Gas Scattering

L. I?. LeClair[†] and S, Trajmar

Jet Propulsion Laboratory, California Institute of Technology,

Pasadena, CA, 91109, USA

M.A. Khakoo

Department of Physics, California State University, Fuller[on, CA, 92634

J.C. Nickel

Department of Physics, University of California, Riverside, CA, 92521

[†] National Research Council Resident Research Associate

P.A.C.S. # 34.80. Gs

Abstract

We describe a crossed electron beam-atomic beam apparatus which utilizes a pulsed electron gun and field free drift tube to obtain time-of-flight (TOF) spectra of electrons scattered from atoms and molecules. This apparatus was constructed for the purpose of obtaining inelastic to elastic differential cross section (DCS) ratios in the energy range extending from threshold to several eV above the threshold of the inelastic channel. The TOF approach eliminates the need for complicated calibration procedures required in conventional electron scattering experiments employing electrostatic lenses and energy anal yzers. The characteristics of the apparatus will be given, along with representative TOF spectra from carbon monoxide. From the spectra we obtained DCS ratios at 90° scattering angle for excitation of the $a^3\Pi$ state of CO, in the impact energy range of 6 to 15 eV.

I. INTRODUCTION

A. Brief Background

Differential cross sections (DCS 's) for electron scattering from gases are required for the detailed understanding and modelling of electron interactions with various atomic and molecular species. Examples of such phenomena are found in electric discharges, plasmas, and the upper atmosphere. Even though there has been considerable effort expended to obtain DCS measurements from a multitude of target atoms and molecules for all electron impact energies, there remains one outstanding problem: no reliable and convenient means have be found to measure absolute inelastic DCS's at impact energies near threshold. Low energy experimental results are particularly needed to evaluate various theoretical approaches aimed towards DCS calculations, since the approximations used for DCS calculations at high impact energies no longer work near threshold, making the numerical calculation mom complicated and difficult.

The success achieved in DCS measurements has been two sided. On one hand, elastic DCS measurements over a wide range of electron impact energies and scattering angles have been obtained with uncertainties approaching $\pm 5\%$. On the other hand, the success has been more modest concerning inelastic DCS 's. Most of the inelastic measurements have been carried out at electron impact energies lying well above the excitation threshold. As the impact energy approaches the threshold, experimental difficulties arise which bring about large uncertain ies in the measured inelastic DCS's. In what follows, we will summarize the experimental problems involved in measuring inelastic DCS's at electron impact energies near threshold, describe our approach to the problem, and present some results obtained from CO to demonstrate our procedure.

B. The problems in conventional DCS measurements

The inelastic scattering of an electron (e) from an atom or molecule (X) in the ground state can be expressed

$$e(E_o) + X(\text{I. E.} = 0) \rightarrow e(E_r, \theta, \phi) \text{ -t- } X(\text{I.E.} = E_l),$$

where $E_o = E_r + E_i$; E_o is the kinetic energy of the incident electron; E_r is the residual kinetic energy of the outgoing electron; and E_i is the energy lost from the electron which has gone to exciting the atom or molecule and raising its internal energy (I.E..). θ is the polar angle that the outgoing electron makes with respect to the trajectory of the incoming electron, and ϕ is the azimuthal angle measured around the axis made by the trajectory of the incoming electron. In most experiments the target molecules and the spin vectors of the incoming electrons are randomly oriented, thus there is no azimuthal dependence. Note that the outgoing electron may not be the same as the incoming electron.

DCS measurements are usually carried out with electrostatic Electron Energy Loss Spectrometers (EELS). in an EELS experiment, a well defined, nearl y mono energetic beam of electrons of nominal energy E_o is directed towards a gaseous target, A detector is placed at an angle θ with respect to the incident beam and detects electrons over a small angular range around the nominal θ. The detector has an electrostatic energy analyzer. It is used to select a certain energy of scattered electrons (E,), corresponding to the excitation of a speci fic energy level i in the. target molecule. The count rate from the detector, I_i (E_o, θ) can be related to the DCS for that channel by the following equation (after some approximations):

$$I_i(E_o, \theta) = DCS_i(E_o,\theta)\, F(E_r)\, G(V)\, I_o . \tag{1}$$

Note: we distinguish here the measured differential cross section(DCS), which always represents some averaged value over the energy and angular resolution of the apparatus, from the differential cross section $\partial\sigma/\partial\Omega$, which refers to a unique E_o and θ. In equation (1) I_o is the incident electron beam current (in particles per second), and F is the instrumental response function (IRF) of the detector, and is dependent on the residual energy of the scattered electrons. G depends on the finite volume defined by the overlap of the electron and target gas beams which lies in the field of view of the detector. It is given by the integral

$$G(V) = \int_V n(\vec{r})\, f(\vec{r})\, \Delta\Omega(\vec{r})\, d\vec{r} \tag{2}$$

4

where n is the number density of the target gas, f is the function which describes the spatial distribution of electrons in the beam, normalized to unity, and $\Delta\Omega$ is the solid angle subtended by the entrance to the detector with respect to the point $\vec{r}$ (see Ref. 1 for more details).

'I'he difficulty in measuring a DCS lies in obtaining F and G. They require a precise knowledge of the spatial distribution of the gas density, the flux distribution in the electron beam, the scattering geometry, and the overall IRF, which includes transmission factors in the electrostatic lenses and energy analyzers, and the quant urn efficiency of the electron multiplier typically used in these experiments. In addition, those factors must be kept free from drift during the long acquisition times necessary to get meaningful data. All of these requirements are difficult to satisfy at low impact energies. The most accurate absolute DCS's measured so far are those for elastic scattering by He. Thus, He has been extensively used as a standard from which elastic DCS's for many other atoms and molecules have been measured, by means of the relative flow technique.[2,3] The utilization of elastic DCS's to get inelastic DCS's is hindered by F.

In a typical measurement of an inelastic DCS for a channel i in an EELS experiment, E_o and θ are fixed, while E_i is scanned over a range that includes the elastic channel ($E_r = E_o$) and the energy loss channel i. The inelastic DCS can be found by taking ratios of the count rates for both processes, and so from (1) we have

$$\frac{I_i(E_o,\theta)}{I_{el}(E_o,\theta)} = \frac{DCS_i(E_o,\theta)}{DCS_{el}(E_o,\theta)}\frac{F(E_r)}{F(E_o)} \tag{3}$$

where the subscript el refers to the elastic channel. Provided one has the elastic DCS for the gas under study, the determination of F is all that remains. At high impact energies, and therefore high residual energies, F does not vary significantly with the residual energy and the F ratio is approximate] y unity. However, at low residual energies, the F ratio can vary quite drastically within a few eV. It depends on a complex interplay between electrostatic lens aberrations, surface conditions present in the energy analyzer, and the electron impact energy. F must be determined empirically during the course of the experiment, ideally under the same conditions that the data was taken. Several means to measure F have been devised, but these

have their limitations[3,4]. So far, no reliable and convenient solution to this outstanding problem "
has been devised.

C. The time-of-flight approach

Our approach to this problem was to eliminate the electrostatic energy analyzer and the
associated collection optics altogether and replace them with a field-free drift tube. By pulsing
the incident electron beam, we observed time-of-flight (TOF) spectra of the scattered electrons.
Instead of dispersing the scattered electrons in space according to their energy, they were
dispersed in time. Under proper operating conditions, the inelastic to elastic scattering intensity
ratios obtained from the TOF spectra are equivalent to the corresponding DCS ratios. As there
were no electrostatic optics these intensity ratios should be independent of residual energy,
impact energy, and scattering geometry. In other words, the F ratio in equation (3) was reduced
to unity.

The advantages of the TOF approach for electron impact experiments, (i.e. its simplicity,
and its potential to detect electrons with equal efficiency no matter what their energy, even sub
eV energies) have been noted in earlier studies. Those. efforts were mainly concerned with the
study of electrons ejected following electron impact ionization of atoms and molecules at high
impact energies[5,6] or low energy electron impact ionization.[7] The TOF approach has also been
used to a great extent in order to obtain total cross sections for electron scattering at sub eV
energies,[8-11] but those are concerned with electron transmission through static gases. Our work
is the first application of TOF electron spectroscopy to the measurement of DCS ratios for
inelastic scattering in a crossed beam experiment. Preliminary reports of this work have been
presented at conferences. [12,13]

6

II. APPARATUS

A. General description

The apparatus (see figure 1) consists of a simple electron gun and a 20 cm long drift tube, oriented at 90° with respect to each other. The gun and the drift tube are placed in a double magnetic shield inside a large vacuum chamber. The double magnetic shield was necessary in order to meet the stringent field requirements for TOF spectroscopy of low energy electrons[8]. We were able to reduce the field strength to 1 to 2 mgauss after degaussing the internal shield. The degaussing was applied after the vacuum chamber was closed. The vacuum was maintained by a 25 cm diffusion pumped charged with Santovac® oil, and reached a base pressure of 1×10^{-7} torr. A liquid nitrogen trap was used to reduce backstreaming from the diffusion and mechanical pumps. In order to maintain the cleanliness of critical surfaces, the entire apparatus was operated at 150 C, using hi-coaxial resistive heaters which have virtually no magnetic field. The construction materials were aluminum and molybdenum, and brass screws were used as fasteners. Care was taken so that no aluminum pieces or brass screws were exposed to electrons. Two faraday traps were placed as shown to reduce the intensity of reflected electron pulses in the TOF spectra. The target gas beam emanated from a molybdenum capillary tube.

B. The pulsed electron gun

The simple electron gun was designed using the electrostatic lens tables of Harting and Read[14]. Some modelling of the electron gun was also carried out using the ion trajectory program SIMION[15]. Our design requirements called for a highly collimated beam of at least 100 nA at 5 eV. The actual gun was built out of aluminum components for economy, but all apertures and deflectors were made from molybdenum. Aluminum surfaces exposed to the electron beam were painted with Aquadag®. A thoriated tungsten hairpin filament was used as the electron source, with the initial beam formed by a Pierce element. Referring to figure 1, lens 1 (J.1) focusses the beam onto the skimmer aperture. After passing through the skimmer, lens 2 (1.2) focusses the electron beam onto the target gas beam. The three short deflector plates

were used for aligning the electron beam with the apertures in the electron gun. The longest deflator plates were used to create the pulses of electrons. The electron gun performed very well, producing up to 200 nA of current in the d.c. mode at energies as low as 2 eV. The diameter of the electron beam at the interaction region was approximate] y 1-2 mm over the energy range used in the experiment, as measured by scanning a slit across the electron beam. We should point out that our electron gun was designed and operated so that the kinetic energy of electrons passing between the longest plates was 20 eV for any electron impact energy (E_o).

The method of producing short pulses of electrons by sweeping an electron beam across an aperture has been reviewed many times before. We refer the reader to the excellent exposition of the physical principles in the article by Bakker[16], which covers the case where the riseti me of the deflecting voltage is faster than the time taken by the electrons to pass between the plates. From Bakker's analysis, the width of a pulse, t_p, produced by sweeping an electron beam of diameter B across an aperture of diameter A is given approximately by

$$ t_p \qquad \text{'} \qquad \frac{A + B}{(eV_o/m_e S)(2t_1^2 + 4t_1t_2 + 4t_2^2 - \frac{1}{3}t_r^2)^{1/2}} \qquad (4) $$

where e is the electron charge; V_o is the voltage between the plates which deflects the electron beam away from the aperture at the start of the sweep (it is reversed by the completion of the sweep); m_e is the electron mass, S is the separation of the plates; t_1 is the transit time of the electrons through the plates; t_2 is the transit time of the electrons from the exit edge of the plates to the aperture; and t_r is the risetime of the sweeping voltage. According to the geometry of our design (S = 8 mm, length of plates = 3 cm, distance from plates to aperture=5 mm) we calculated t_p = 1.9 ns using a deflection voltage of 2.5 V which is reversed by the end of the 5 ns sweep. This amounts to about 1200 electrons per pulse for a 100 nA electron beam.

We initially used the sweeping method to produce the electron pulses, but a peculiar problem arose. We swept the beam back and forth across the aperture with a square pulse of 5 to 10 volts, having a rise time of 5 ns. The pulse was capacitively coupled to the deflection plate through a 10" nF capacitor, as shown in figure 1. This of course produces two electron pulses per cycle. The peculiarity was that TOF spectra from pulses produced by the outgoing

8

sweep were different in structure from those produced by the return sweep.   Further investigation indicated that the electron impact energy had shifted from the calibrated value (see below) for both the outgoing and the return sweep pulse by 1-2 eV, depending on the amplitude of the applied electric pulse. The energy shift was higher than the calibrated value on the outgoing sweep, and lower on the return.   This indicated that an axial electric field component was present in the deflector during the sweeping, possibly due to fringe fields and/or the inhomogeneous electric field components between the plates.   We took no special design considerations with the deflection plates to eliminate fringe effects.

To circumvent this problem, we opted to pulse the electron beam by the toggle method. In this case, the electron beam is deflected to one side by a d.c. voltage, and a triangle pulse with an amplitude equal to the deflection voltage is applied. A sufficient y short triangle pulse would result in electron pulses comparably short to those obtained by the sweep method, with little loss in resolution. The average electron impact energy of these pulses was found to be identical to that obtained by calibration (see below). At the peak of the triangle pulse there is no electric field, and so, no temporal axial gradient to accelerate the electrons. We typically used triangle pulses 2 to 3 volts in amplitude, with a risetime of 10 ns.

When pulsing an electron gun, the elements will pick up the pulse though capacitive coupling, usually resulting in a "ringing" of the elements' voltage on the up or down transition of the applied electric pulse. To remedy this, one attaches capacitors between every element and the ground (i.e. the wall of the vacuum chamber). In our case, we used 0,01 μF ceramic disc capacitors, which reduced the ringing to less than 20 mV in amplitude on every element. This small "ringing" voltage could not account for the energy shift we observed when using the sweeping method to produce pulses.

C. Calibration of the electron impact energy

To calibrate the electron impact energy, we built a neutral metastable particle detector, similar to one which has been described previously.[17] It was simply a box containing a 1 cm square piece of tantalum, which is heated to 200 C to maintain a clean surface, and a Spiraltron® electron multiplier (Galileo model 4219). There is a hole in the box to expose the tantalum to the interaction volume created by the intersection of the electron and gas beams. Biased grids

cover the hole in order to keep out electrons and ions.   Adjacent to the tantalum is the open mouth of the Spiraltron® which is biased at +-200 V with respect to the grounded tantalum. Metastable particles with an excitation energy greater than the work function of the tantalum (4. 1 eV) are detected when they impinge on the tantalum and eject electrons by auger emission.

Calibration was accomplished by operating the electron gun in the d.c. mode, ramping the impact energy, and acquiring the count rate of metastable particles with a multi-channel scaler.   For example, when working with CO, we measured the threshold for $CO(a^3\Pi)$ production at 5.1 ± 0.2 V, indicating a contact potential of 0.9 eV, since the excitation energy of $CO(a^3\Pi)$ is 6.01 eV. $CO(a^3\Pi)$ has a lifetime of several milliseconds, depending on its vibrational state. Our metastable detector was placed 30 cm from the interaction region, directly in the beam of gas effusing from the capillary tube. This was close enough to produce a good count rate. This arrangement also worked well with He, even though most He metastables recoil significantly following electron impact.

Another means to calibrate the electron impact energy scale comes from the TOF spectrum itself.   We calibrated the time scale in the TOF spectrum with a high-accuracy, precision digital delay generator (SRI Model DG535). By measuring the time between two sharp features in a TOF spectrum (i.e. using He as the target gas) and knowing the energy levels they correspond to, we calculated a contact potential of 0.9 eV, confirming our result for He from the metastable detector. Note, as stated earlier, that this was the case only when we used the toggle method to produce electron pulses.

D. The interaction region

The interaction region was enclosed in a box formed out of molybdenum sheet metal, and was kept at ground potential, The top of the box was open to allow the gas beam to be pumped away, and expose the metastable detector to the interaction volume. The gas beam was formed by a 6 cm long molybdenum capillary tube with an internal diameter of 1 mm. It protruded vertically from the bottom of the box, and was in good electrical contact with the box. The driving pressure behind the capillary was typically about 1 torr. The orifice of the capillary tube was 6 mm below the electron beam. The intersection of the electron and gas beams takes place 2.5 cm from both the exit and entrance apertures of the electron gun and drift tube.

10

opposite to the exit aperture for the electron gun, at a distance of 25 cm, was a box which functioned as a faraday trap to collect the electron beam. Its opening was covered with molybdenum mesh, and the collector plate inside the box was biased by +45 V with respect to ground. We found this necessary because without a bias on the collector plate, an echo of the incident electron pulse would appear in the TOF spectra; with a bias the echo was reduced by 80%. It is probably possible to reduce the echo even more by using a longer faraday trap, but we were limited in space. Opposite to the entrance aperture of the drift tube, at a distance of 10.0 cm is another faraday trap like the one just described. Its function is to remove the echo from TOF spectra caused by electrons which scatter elastically from the target gas and bounce off of the wall of the magnetic shield back into the drift tube. While it was not possible to completely remove the echo pulses from TOF spectra, we measured their contribution to be less than 0.5 % of the inelastic intensity, at worst.

E. The TOF drift tube

'l<here have been many TOF spectrometers made primarily for photo-electron studies. Often these have some means of magnetic or electrostatic focusing so that all of the emitted electrons can be collected. Our goal was to collect only those electrons which scattered into the solid angle defined by the apertures of the drift tube. There must not be any fields in either the interaction region, or in the drift tube. However, it must be pointed out that even in the cleanest vacuums, patch fields can form on metal surfaces which are strong enough to significantly alter the trajectories of electrons with less than 1 eV of kinetic energy.

Our drift tube was constructed out of aluminum, but its inner walls were lined with sheet molybdenum 0.1 mm thick, and the apertures were made from the same material. We designed the experiment in such a fashion that once electrons enter the box that surrounds the interaction region, the only surfaces they were exposed to at close range. (for up to 20 cm) were made of molybdenum. Electrons which scattered into the drift tube continued to "see" only molybdenum until they reached the multi-channel plates. All of the. molybdenum pieces were pressed tight together to form one continuous unbroken surface, and this surface was grounded to the vacuum chamber wall. The use of one metal eliminates contact potentials detrimental to the collection of low energy electrons.

11

We feel that a few comments should be made on the choice of rnol ybdenum. It has been our experience (and that of others studying low energy electron scattering from gaseous targets, [18,19] that molybdenum is in general resistant to chemical reactions that can take place in the presence of gaseous targets and electrons. Thus, it is least susceptible to contamination and has the weakest patch fields of any metal. The use of colloidal graphite coatings (such as AquaDag® or AeroDag® G, available from the Acheson Colloid Company in Michigan, USA) on metal to reduce patch fields is common. However, both of these colloids contain non-conductive binders, and whether or not these binders can form patch fields that effect low energy electrons, especial] y when the apparatus is baked, appears to remain an unanswered question. One group has reported[20] that bare molybdenum surfaces work fine for low energy electron work, provided the target gas is fairly inert, but a coating of AeroDag® over the molybdenum is necessary when the target molecules are reactive. Ibach has described a high performance EEL spectrometer for use in surface science. [21] It was made of copper, and coated with colloidal graphite in order to reduce patch fields. It has a reported resolution of just under 1 meV, demonstrating the effectiveness of the solution. However, it has not yet been demonstrated if this resolution can be attained for experiments on electron scattering from gaseous targets, where the background pressure is higher, by several orders of magnitude, than that used in surface studies; and where the low density of the target gases necessitates the use of electron beam currents that are higher than those used in surface science.

The molybdenum in our apparatus was carefully cleaned in the following manner prior to assembly. It was scrubbed with an abrasive metal cleanser (Bar Keeper's Friend", which contains oxalic acid) using extra fine grit abrasive scrubbing pads (ScotchBrite®); rinsed in tap water; given an ultrasonic bath in a metal cleaning soap solution (Alfa-Kleen®); rinsed in tap water; then in distilled water; and finally blow dried with oil-free compressed air. Once assembled and under vacuum, the apparatus was baked for at least two days to remove all water contamination.

At the end of the drift tube, the electrons must pass through a "slat grid" constructed from strips of molybdenum. The "slat grid" separates the field free drift region from the post acceleration region. It is better than using an ordinary grid for the same purpose since the presence of the latter will create transverse components of the electric field which deflect low

energy electrons[8]. In addition, it is easy to clean. The strips were separated by a distance equal to one fifth of their width (1.6 cm), reducing field penetration by a factor of 1000.

Once pass the "slat grid", the electrons find themselves in the post acceleration electric field created by the 450 V bias on the surface of the first multi-channel plate (MCP, from Galileo). We choose a voltage large enough so that the detection efficiency was virtually independent of residual energy for the range of impact energies in this experiment. [5] We used three stacked MCP'S to produce large output pulses. Each MCP has an active surface area 40 mm in diameter, with a 0.5 mm gap between each plate. A resistor ladder network was used to supply the bias voltages to the MCP's, similar to an arrangement described earl ier.[7] Our resistor ladder was made from ordinary 0.5 watt carbon resistors, and placed behind the MCP assembly in the vacuum. The bias voltage across each MCP was approximate] y 900 V. We operated at a background pressure around 6×10^{-6} torr (calibrated by the ionization efficiency factors for ion gauges[22]) for months without any noticeable effect on the MCP'S, even though they are not recommended for operation above 2×10^6 torr.

The apertures in the drift tube define a solid angle with an apex of 6.4° at the intersection of the electron and gas beams. The distance from that intersection to the front of the slat grids was 20.0 cm; the distance across the "slat-grid" was 1.6 cm, and the distance across the post-acceleration region was 1.4 cm. We calculated the TOF of the electrons by assuming field free drift through the slat grids, and a uniform post acceleration field. The former gave a TOF (in ns) of $364/\sqrt{E_r}$ where E_r is the residual energy in eV. The time in post-acceleration was virtually the same for all residual energies up to 10 eV, about 2.0 ± 0.1 ns.

F. Electronics

Voltages to the electron gun were supplied by a bank of potentiometers. Pulses for the deflector plate were delivered by a Hewlett-Packard 8111A Pulse Generator. TOF spectra were acquired using an Ortec 437A Time-to-Amplitude Convertor (TAC) in conjunction with a Nuclear Data 62 Multi-Channel Analyzer. Both the pulser and TAC were started by a home-built pulser operating at 100 KHz. We operated at count rates that were low enough (less than 500 Hz) to avoid TAC pile up . Pulses from the MCP's passed through two cascaded pre-arnps (Avantek GPD 401) and a Constant Fraction Discriminator (EG&G Ortec 934) before being fed

to the stop of the TAC. The pulses from the MCP's had a risetime of about 1 ns, with a bit of overshoot on the falling edge.   No geometrical measures were taken towards impedance matching the MCP output to the coaxial cable (as is found in some ultra fast applications[23]) since a timing resolution of 1 ns was sufficient for our needs.

G. Resolution

There are several factors which contribute to the resolving power of a TOF electron spectrometer. Those which contributed the least in our instrument include the finite width of the interaction volume, weak electric and magnetic fields, space charge, and time resolution, The two dominant factors in our instrument were the energy spread of the incident electron beam, and the pulse width.

Let us consider first the energy spread of the electron beam. A pulse, which leaves the skimmer, will broaden as it travels away from the skimmer because of the energy distribution of electrons emitted by the thermionic source.   Even though equation (4) was derived for a rnonoenergetic beam, we can approximate the broadening of the pulse width due to the energy spread by treating the resulting dispersion separately. Let t_d be the time broadening due to this dispersion. The time, t (in ns), it takes for electrons of energy E_o (in eV) to travel a distance d (in cm) is given by $t = 16.87 d / \sqrt{E_o}$. A packet of electrons with an energy distribution having a FWHM given by δE, all starting at $t=0$, will spread out into a packet of width

$$ t_d = 8.44 d \, \frac{\delta E}{E_o^{3/2}} \, . \tag{5} $$

Thus, if the packet has an initial temporal spread given by (4), then we can expect that pulses at a distance d to have a temporal spread given by $t_p + t_d$. Assuming a quasi-Maxwellian energy distribution in our beam, with a full-width-half-maximum (FHWM) about 0.6 eV (typical of thermionic sources), a pulse of 10 eV electrons will broaden by an additional 1.7 ns at the interaction volume in our apparatus.   The sum of equations (4) and (5) serve as an ideal limit to the pulse width. Thus, in our example, the FWHM of the pulse at the interaction region will be almost 4 ns wide, if using the sweep mode. We can expect nearly the same result with the

14

toggle mode. There will probably be some additional broadening due to the fringe fields of the deflection plates and the electric fields in the final deceleration stage of the electron gun.

The resolution of our TOF electron spectrometer can be calculated by application of equation (5) to the electrons scattered into the drift tube. Consider two features in a TOF spectrum at times t' and t'' corresponding to electrons with residual energies E_r' and E,", We will consider the two features to be just resolved if they are separated in time by an amount equal to half the sum of their FWHM's. If we make the approximation that $|t'-t''| < (t' + t'')/2$, and let $E_r' \approx E_r'' \approx E_{av} = (E,' + E_r'')/2$, then the minimum energy separation that can be resolved, ΔE_{min}, is given approximately by

$$\Delta E_{min} \approx \frac{F_{av}^{3/2} t_w}{8.44D} + \delta E \tag{6}$$

where t_w is the width of the pulse at the interaction region (calculated from equations (4) and (5)), and D is the length of the TOF drift tube. Equation (6) makes physical sense. No matter how much we shorten the pulse or increase the length of the drift tube, the resolution is limited by the energy spread of the incident electron beam. In addition, the energy resolution becomes worse for high E_{av}, that is shorter flight times.

As an example, consider a TOF spectrum of electrons scattering from CO with $E_o = 10$ eV. Electrons which excite the $CO(a^3\Pi)$ and $CO(A^1\Pi)$ states will consequently have an average residual energy of about 2.5 eV. This gives a resolution of 0.7 eV, which leaves plenty of room to separate the two features, but the vibrational structures will be unresolved.

III. EXPERIMENTAL RESULTS

A. Spectra, intensit y rat ios, and cross sections

Two TOF spectra of electrons scattered elastically from a gaseous target are shown side by side in figure 2 for $E_o = 2$ and 5 eV. In each case t_d was calculated using equation (5) with $d=3$ 1.6 cm (distance from the skimmer in the electron gun to the end of the field-free drift) and

$\delta E = 0.6$ eV, and subtracted from the measured FWHM. The difference between the measured FWHM and t_d was about 3 ns at 5 eV, but this increased to 8 ns at 2 eV. The lower value of the difference probably is a good indication of the actual pulse width at the skimmer. The higher value at 2 eV is probably due to broadening that occurs as the electron pulse is decelerated from 20 eV at the skimmer to 2 eV in the interaction region. A common feature to the pulses in figure 2, and those obtained at other impact energies, is the remarkably good fit to a gaussian function (using the least squares method). The gaussian shape of the pulses is a result of the convolution of several factors; notably the energy spread of the electrons and the radial profile of the electron beam at the skimmer.

Figure 3 shows TOF spectra obtained from CO (99.99% purity, Matheson) for various impact energies. We chose CO as the first candidate of study for several reasons: (a) the lowest lying state, $CO(a^3\Pi)$, is easily resolved from other states; (b) a detailed and painstaking measurement of the DCS for electron impact excitation of the $a^3\Pi$ state at near threshold energies was being carried out concurrent] y by another Zobel et al. [24] using a conventional electrostatic EEL; and (c) CO is an important astrophysical molecule. In figure 3 one can see the elastic peak and the inelastic features due to excitation of $CO(a^3\Pi)$, $CO(A^1\Pi)$, and the ionization continuum. Note that the background in each spectrum is flat. In addition, the background count rate was three to four orders of magnitude lower than the maximum for the inelastic features. This indicated very little leakage of electrons from the electron gun when in the off mode. Each spectrum took approximately 30 minutes to acquire.

We define the ratio, R, to be the intensity of the feature due to excitation of $CO(a^3\Pi)$ divided by the intensity of elastic scattering. Determination of the intensity of each feature was straight forward for $E_o < 10$ eV. At 10 eV and higher the $A^1\Pi$ feature began to overlap with the $a^3\Pi$ feature. It became necessary then to employ a computer program to unfold individual intensities by fitting up to five gaussians to each feature. This worked well, but we did not go beyond $E_o = 15$ eV because of the increasing uncertainty. The ratios have been tabulated in Table 1. The ratios were checked for linearity with respect to electron beam current and target gas pressure. We found no detectable departures from linearity for d.c. electron beam currents up to 200 nA (the limit of our gun) and background gas pressures up to 1×10^{-5} torr. Our measurements were taken at 160 nA d.c. equivalent current, at a pressure of 6×10^{-6} torr. We have multiplied our ratios by the elastic DCS data of Gibson et al. [25] for CO at 90° (see Table

16

I) to determine the DCS for $CO(a^3\Pi)$ at $90°$. The resulting inelastic DCS data are also tabulated in Table I and plotted in figure 4. We have also plotted the measurements made by Zobel et al .[24] and Middleton et al.[26]; and the theoretical calculations of Sun et al .[27] (which are based on the Schwinger multichannel variational method).

It can be seen that the agreement between the present results and those of Zobel et al. is exceptional y good, except for the 7,5 to 8.5 eV range. The uncertainty in the DCS measurement of Zobel et al. is $\pm$ 24 %. The uncertain y in our measurement at $E_o = 10$ eV comes from adding the uncertainty in R (4 %) with the uncertainty of the elastic DCS measurement (7%) in quadrature to obtain 3:8%. It is significant that two independent methods agree so closely. Because of the nature of the calibration scheme used by Zobel et al., they were not able to extend their measurements beyond 9.7 eV. Extrapolation of our measurement to $E_o = 20$ eV indicates a good agreement with the measurement by Middleton et al. There is also fairly good agreement with the theoretical calculations below $E_o = 10$ eV.

B. Uncertainties in the measurement of R

We cannot resolve the elastically scattered electrons from those which have excited the vibrational levels of the ground state. The contribution of the latter can be neglected since the DCS for this process at $90°$ is almost 3 orders of magnitude smaller than the elastic cross section for our energy range.[28,29] "f'he contribution of electrons which have excited other triplet states near $a^3\Pi$, namely the $a'^3\Sigma^+$ and d^3A states, can be also be neglected since their energy loss features overlap more with the $A^1\Pi$ feature and the DCS's for excitation of theses states are at least 2 orders of magnitude smaller than the DCS for $a^3\Pi$[24]. The contribution from scattering by the background gas to the elastic peak was found to be less than 0.5%. The intensities in the TOF spectra were large enough to reduce the statistical uncertainty to about 0.4%.

The largest error in R (for certain energies) came from day to day variations of about 3%. The source of the variation appeared to stem from the beam steering of the final deflector plates. For each measurement of R the final deflector plates were adjusted to maximize the intensit y of the metastable signal measured by the warm tantal urn detector. While this maximized the electron beam overlap with the gas beam, wc could not be sure that the angle between the incoming electron beam and the axis of the TOF tube was precisely $90°$, but

17

estimate that it was within 10. This variation was worse around $E_o = 9$ eV, presumably since the DCS of $CO(a^3\Pi)$ varies steep] y with angle at 90° (Zobel et al., 1995), at that energy. We also found that R could be made to vary by a few percent by changing the focus of the final lens, 1.2. When measuring the ratios, the focus of 1.2 was always adjusted in order to maximize the intensity of the metastable signal. The result of the focussing action is that the trajectory of each electron through the interaction region is not exactly at 90°to the axis of the TOF drift tube, but (ideally) the average angle of all trajectories should be close to it. We found that by defocusing the beam slightly, we could increase or decrease the ratios by a few percent, which indicated that the electron beam was not entirely uniform over its radius. There were two focussing modes of L2. The strong *mode* resulted in a small overlap with the interaction region, but a large spread of angles, which lead to a greater variation in the R. We used the weak focussing mode, where the spread of angles was much smaller, even though the beam was wider. The day-to-day adjustments of the beam steering voltage and the focussing voltage probably occurred because of the gradual contamination of the electrostatic elements by oil vapors which escape trapping. In fact, we found that over a few of weeks the ratios would decrease by 10%. At this point we would disassemble the apparatus and clean it. The ratios were repeatable once the experiment was again underway.

Another contribution to the uncertainty of our ratios in Table I came not from the experiment, but has to do with unfolding the $a^3\Pi$ feature from the $A^1\Pi$. At energies above 10 eV, the uncertainty in R grew larger, to about $\pm$ 10% at $E_o = 15$ eV. This estimate was based on our confidence in the computer program used to unfold the features in the TOF spectra, as determined by unfolding artificial spectra where the ratios were known.

IV. CONCLUSIONS

We have demonstrated for the first time that accurate determination of inelastic to elastic scattering intensity ratios at low electron impact energies are possible with TOF spectroscopy. Utilizing these ratios together with elastic DCS's yields very accurate inelastic DCS'S without the need for troublesome calibration techniques used in conventional electrostatic EEL spectroscopy. In turn, these DCS's can be used as secondary standards to normalize other

18

inelastic DCS's obtained from measurements with electrostatic EEL spectrometers. Now that this simple technique has been demonstrated, the next step is to make measurements over a range of angles, and to use an electron gun with a narrower energy distribution.

ACKNOWLEDGEMENTS

REFERENCES

[1] S. Trajmar and J.W. McConkey, in Adv. At, Mol. Opt. Phys. 33, 63, ed. by M. Inokuti
        (Academic Press, San Diego, 1994)

[2] S.K. Srivastava, A. Chutjian, and S. Trajmar, J. Chem. Phys. 63, 2659 (1975).

[3] J.C. Nickel, P.W. Zetner, G. Shen, and S. Trajmar, J. Phys. E: Sci. Instrum. 22, 730 (1989)

[4] M. Allan, J. Phys. B: At. Mol. Opt. Phys. 25, 1559 (1992)

[5] R.E. Kennerly, Rev. Sci. Instrum. 48, 1682 (1977)

[6] R. Il. Goruganthu, W.G. Wilson, and R.A. Bonham, Phys. Rev. A 35, 540 (1987)

[7] C. Ma, C.R. Sporleder, and R.A. Bonham, Rev, Sci. Instrum. 62, 909 (1991)

[8] G.C. Baldwin and S.1. Friedman, Rev. Sci. Instrum. 38, 519 (1967)

[9] B. Bederson and L.J. Kieffer, Rev. Mod. Phys. 43, 601 (1971)

10 S Trajmar and D. Register, in *Electron-Molecule Collisions,* edited b y I. Shimamura and
        K. Takayanagi (Plenum, New York, 1984), chapter 6

[11] R.I. Gulley, D.T. Alle, M.J. Brennan, M.J. Brunger and S.J. Buckman
        J. Phys. B: At, Mol. Opt, Phys. 27, 2593 (1994)

[12] L.R. LeClair, S. Trajmar, M.A. Khakoo, and J.C. Nickel,
        Bulletin of the Amer. Phys. Sot. 40, 1319 (1995)

[13] L.R. LeClair, S. Trajmar, M.A. Khakoo, and J.C. Nickel, Collected Abstracts from the 19th Int. Conf. Phys. Elect. At. Coil., ed. by J.B.A. Mitchell, J.W. McConkey and C.E. Brion, p. 479 (1995)

[14] E Harting and F.H. Read, *Electrostatic Lens* (Elsevier Scientific publishing, New York, 1976)

[15] D A Dahl and J. E. Delmore, SIMION ver. 4.02 (Report EGG-CS-7233, Idaho Nat. Eng. Lab., Idaho Falls, ID 1988).

[16] J.M.B. Bakker, J. Phys. E: Sci. Instrum. 6, 785 (1973)

[17] M. Zubek and G. C. King, J. Phys. E: Sci. Instrum. 15, 511 (1982)

[18] J.N.H. Brunt, F.H. Read, and G.C. King, J. Phys. E: Sci. Instrum. **10,** 134 (1977)

[19] S.J. Buckman and B. Lohmann, J. Phys. B: At. Mol. Opt. Phys. **19,** 2547 (1986).

[20] G.C. King, personal communication (1995).

[21] H Ibach, *Electron Energy Loss Spectrometers: The Technology of High Performance* (Springer-Verlag, New York, 1991)

[22] J.E. Bartmess and R.M. Georgiadis, Vacuum **33,** 149 (1983)

[23] D.C. Anacker and J. L. Erskine, Rev. Sci. Instrum. 62, 1246 (1991)

[24] J. Zobel, U, Mayer, K. Jung, and H. Ehrhardt, submitted for publication (1995)

[25] J.C. Gibson, L. Morgan, R.J. Gulley, M.J. Brunger, and S.J. Buckman, to be published (1995)

[2] A.G. Middleton, M.J. Brunger, and P.J.O. Teubner, J. Phys. B: At. Mo. Opt. Phys. 26, 1743 (1993)

[27] Q. Sun, C. Winstead, and V. McKoy, Phys. Rev. A 46, 6987 (1992).

[2a] A. Chutjian and H. Tanaka, J. Phys. B: At. Mol. Opt. Phys. **13,** 1901 (1980)

[29] M Tronc, R. Azria, Y. Le Coat, J. Phys. B: At. Mol. Opt. Phys. 13, 2327 (1980)

Table 1. Inelastic to elastic intensity ratios (R) for CO(a³II) as derived from TOF spectra at 90° for various electron impact energies, expressed in percentages. Also shown are the elastic DCS's for CO at 90 °from Ref. 25 in units of 10^{-17} cm^2/ster, and the resulting DCS for CO(a³II) in units of 10^{-18} cm^2/ster. The numbers in parenthesis give the absolute error (3:) for each measurement. Elastic DCS data obtained by polynomial interpolation are denoted by *.

E_o (eV)	R (%)		Elastic DCS	CO(a³II) DCS
6	0	(o)	7.10 (0.48)	0.00 (0.00)
6.5	4.03	(0.3)	6.60* (0.46)	2.66 (0,27)
7	7.58	(0.07)	6.00* (0.42)	4.55 (0.32)
7.5	11.5	(0.2)	5,42 (0.35)	6.24 (0.42)
8	15.7	(0.2)	4.95* (0.35)	7.77 (0.55)
8.5	18.9	(0.5)	4.58* (0.32)	8.66 (0.65)
9	20.9	(0,8)	4.29 (0.28)	8.97 (0.68)
9.5	20.4	(0.8)	4.05* (0.28)	8.24 (0.66)
10	18.4	(0.7)	3.87* (0.27)	7.12 (0.57)
10.5	16.2	(0.7)	3.81* (0.27)	6.17 (0.51)
11	13.9	(0.6)	3.76 (0.25)	5.23 (0.41)
11.5	11.6	(0.5)	3.67* (0.26)	4.26 (0.35)
12	10.8	(0.5)	3.55 (0.23)	3.83 (0.31)
12.5	9.81	(0.5)	3.40* (0.24)	3.34 (0.29)
13	9.17	(0.5)	3.27 (0.21)	3.00 (0.25)
13.5	8.79	(0.5)	3.17* (0.22)	2.79 (0.25)
14	8.37	(0.6)	3.09 (0.20)	2.59 (0.25)
14.5	8.33	(0.7)	2.97* (0.21)	2.47 (0.27)
15	8.23	(0.8)	2.86 (0.18)	2.35 (0.27)

FIGURE CAPTIONS

Figure 1,   View of the TOF apparatus from above. Legend: EG - Electron Gun, DP - deflection pulse, FT - faraday traps, DT - drift tube, MCP - multi-channel plates, L1 - lens 1, L2 - lens 2. The molybdenum capillary tube which forms the gas beam is located at the cross hair, with the flow directed out of the page.

Figure 2..   TOF spectra of the elastic peak for E_o =2 and 5 eV. The solid line is the gaussian fit to the data.

Figure 3.   TOF spectra of from CO which include elastic and inelastic features for various impact energies.   Each spectrum was aligned with the elastic feature, and displaced upwards for clarity.   The zero of the TOF scale is arbitrary.

Figure 4.   DCS for electron impact excitation of $CO(a^3\Pi)$ at 90°. Legend: ● - DCS's derived from our TOF ratios and the elastic DCS data of Gibson et al.[25]; — - Zobel et al .[24]; A - Middleton et al .[26]; O - Sun et al .[27] Representative error bars are shown for the TOF results and those of Zobel et al.
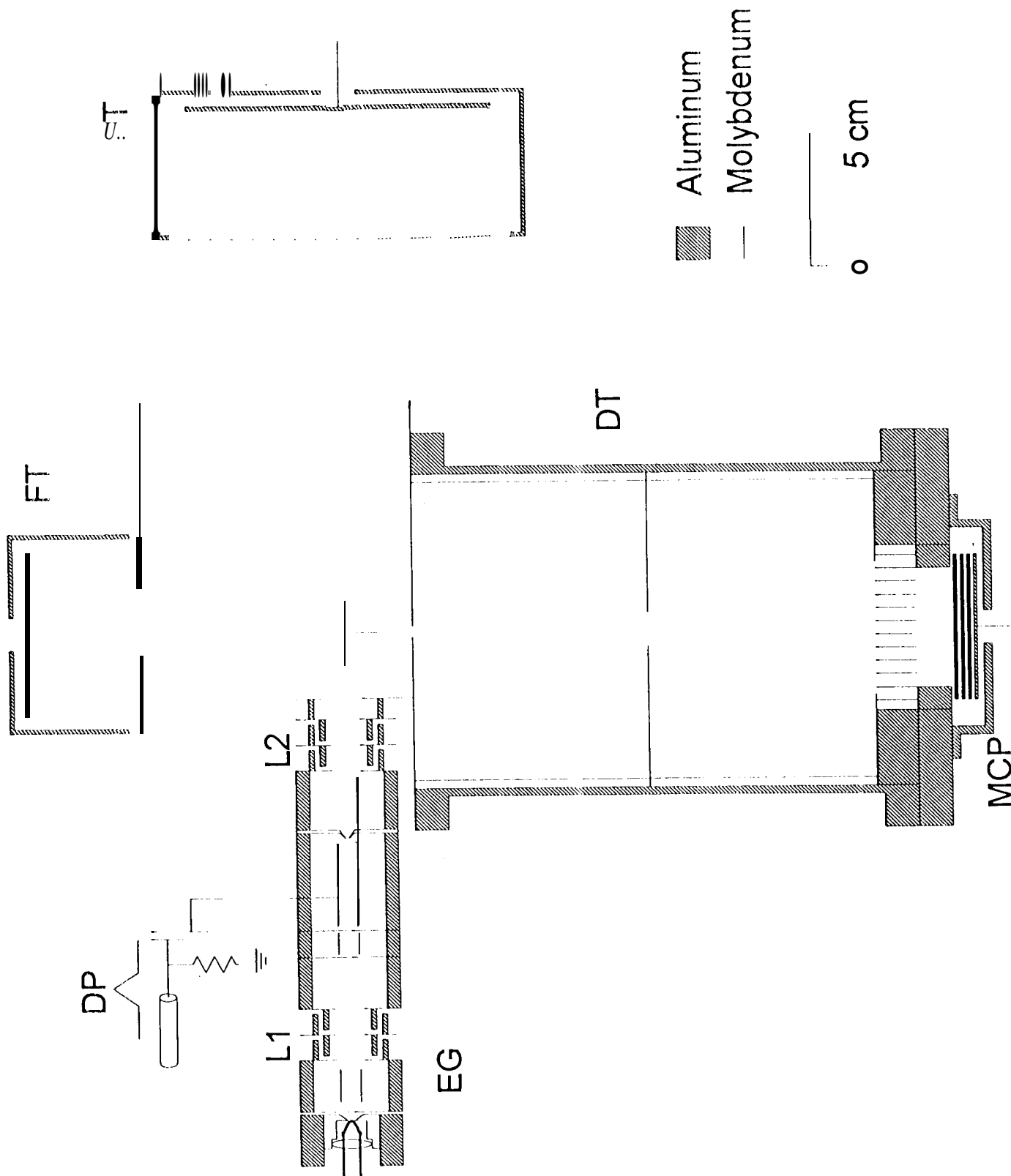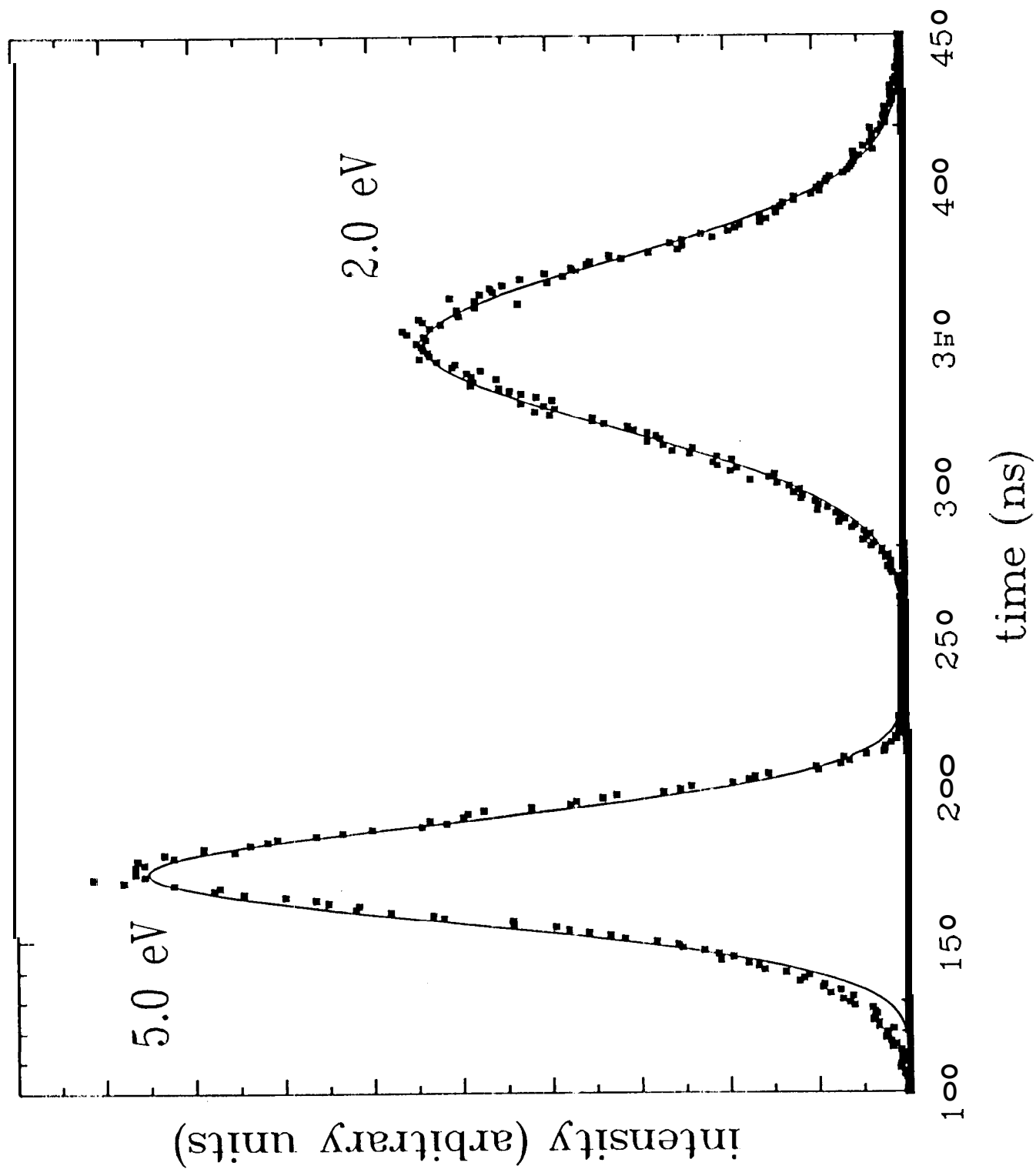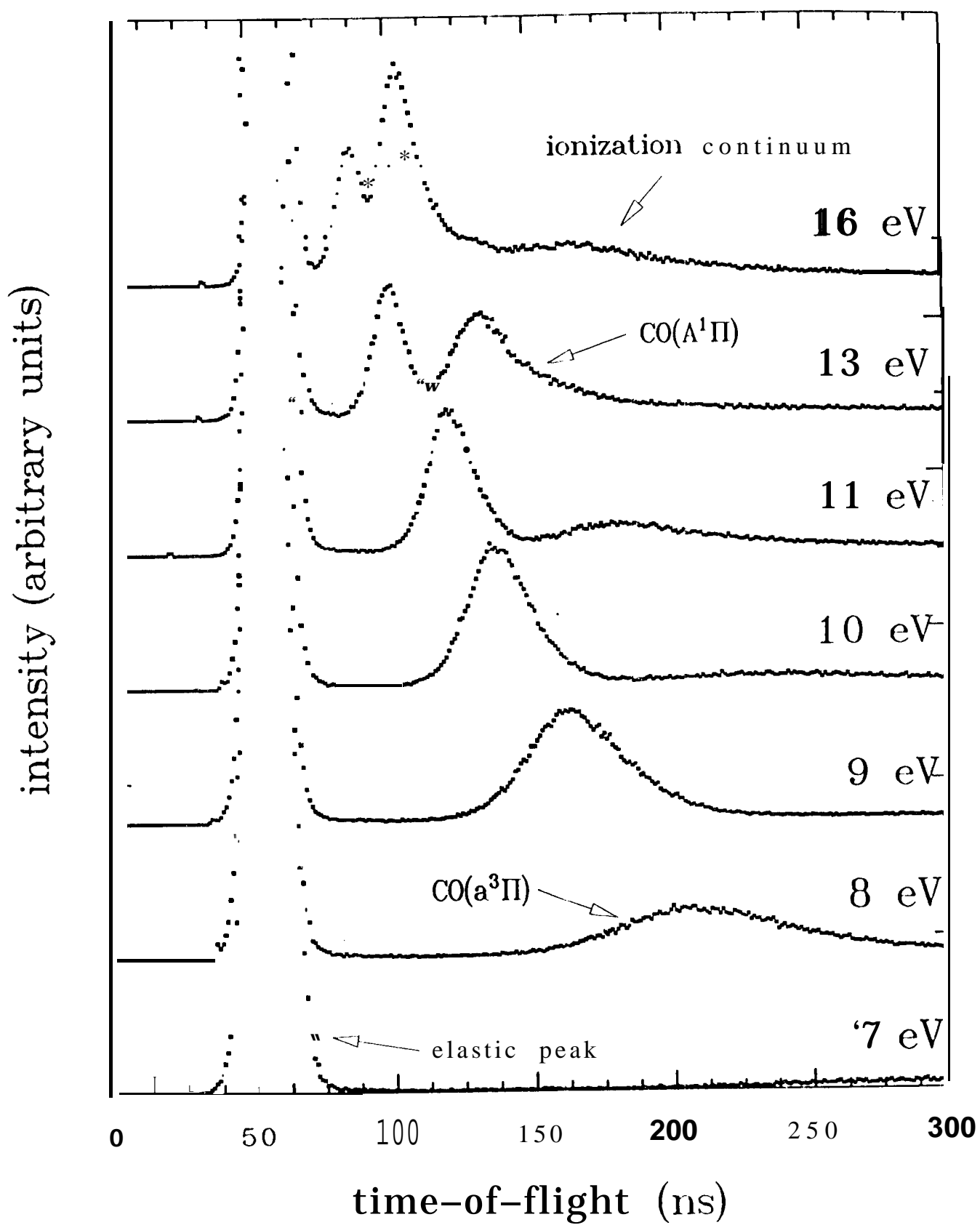
DP

FT

L2

DT

$U_{..}$

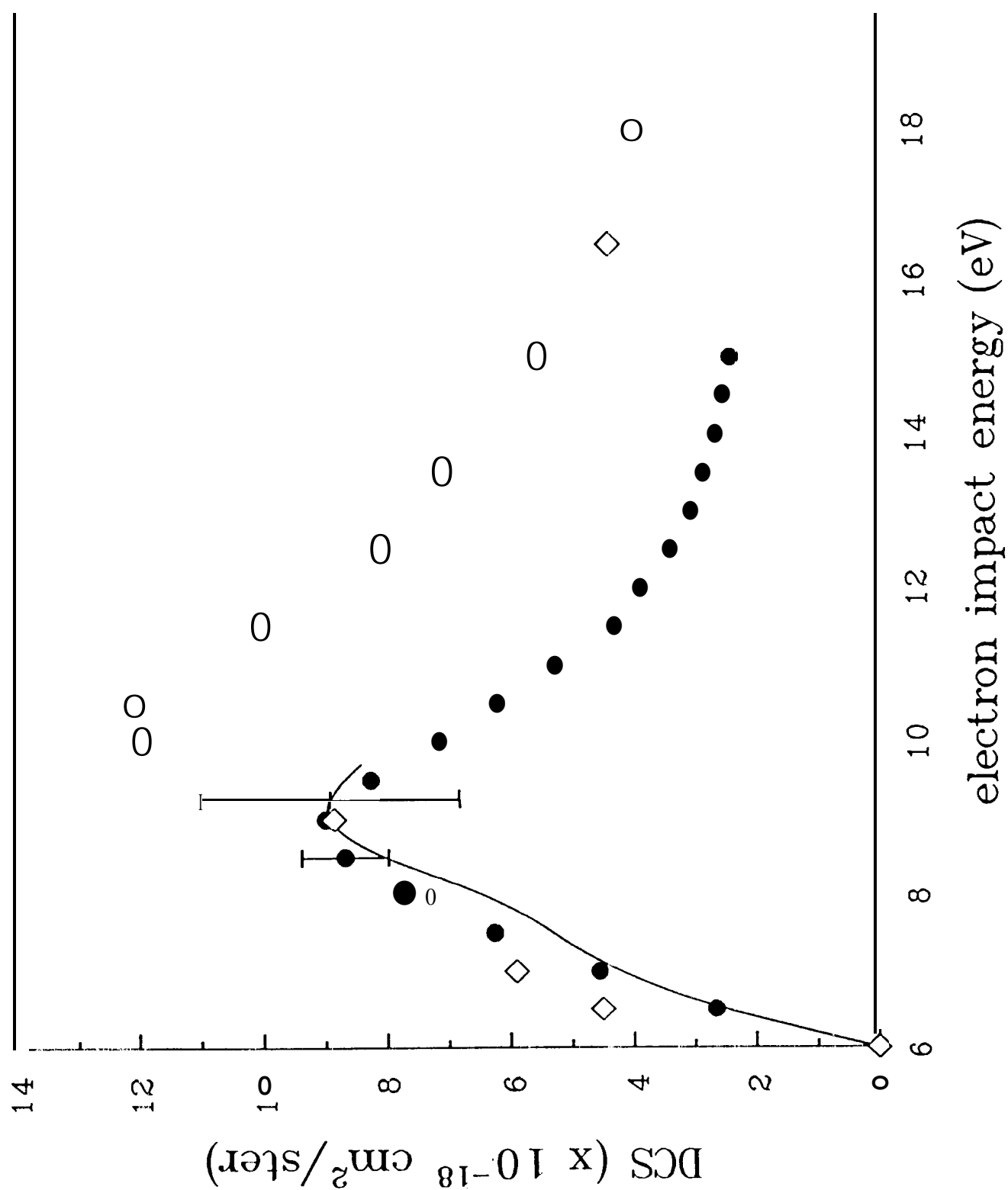Aluminum
Molybdenum

L1

EG

MCP

5 cm

0

Figure 1

Figure 2

Figure 3

electron impact energy (eV)

DCS (x 10^{-18} cm^2/ster)

Figure 4